3D Bearing Capacity of Shallow Foundations Located near Deep Excavation Sites

J.S. Shiau, *Lecturer in Geotechnical Engineering, University of Southern Queensland, Australia*

J.F. Watson, *Research Assistant, University of Southern Queensland, Australia*

ABSTRACT: Foundations are often placed near a proposed excavation site in urban areas and the evaluation of bearing capacity reduction due to the excavation effect is important for geotechnical engineers. This paper aims to estimate the three-dimensional (3D) effect of foundations located near a slope. FLAC3D is used to investigate this problem.

1 INTRODUCTION

The problem of a footing on slope is encountered regularly in engineering practice, with some noteworthy examples being bridge abutments and the tower footings of electrical transmission lines. It is also often the case that foundations are placed near a proposed excavation for the basement construction of high-rise buildings in urban areas.

The slope effects on the bearing capacity of foundations were not investigated extensively. Two dimensional bearing capacity solutions have been studied by Meyerhof (1957), Kusakabe et al. (1981) , Shields et al. (1990) and Narita (1990). Nevertheless their solutions were not complete for a wide range of practical design parameters. Moreover the footing on slope solutions were formulated as modifiled N_c, N_q and N_{γ}. which could be misleading for many design engineers.

Design charts using non-dimensional parameters, such as dimensionless strength ratio, $c_u/\gamma B$, and normalized bearing capacity, $p/\gamma B$, are considered simpler and more useful from a design perspective. Shiau et al. (2008) presented a numerical study of this problem and formulated the solutions as a dimensionless bearing capacity factor. This method is advantageous because trends in the data are very clear and reasonable confidence in design can be achieved using the charts.

There is little literature published for 3D effects. de Buhan P. and Garnier D. (1998) presented some 3D solutions using yield design theory, but their results did not cover a wide range of practical design parameters. Based on the success of Shiau et al. (2008), a FLAC3D model was created to study the 3D bearing capacity of foundations located near slopes. In this paper, 3D results are compared with those in 2D plane strain condition and design charts are presented to facilitate the design.

2 STATEMENT OF PROBLEM

The bearing capacity problem of a rigid foundation resting near a slope is illustrated in Figure 1. The limit behavior of such a rigid foundation system is expected to be influenced by the following parameters:

- Cohesion (c)
- Friction angle (Φ)
- Soil unit weight (γ)
- Slope angle (β)

- Slope height (H)
- Distance from edge of slope (D)
- Length of footing (L)
- Width of footing (B)
- Depth of embedment (D_f)
- Surcharge loading (q)

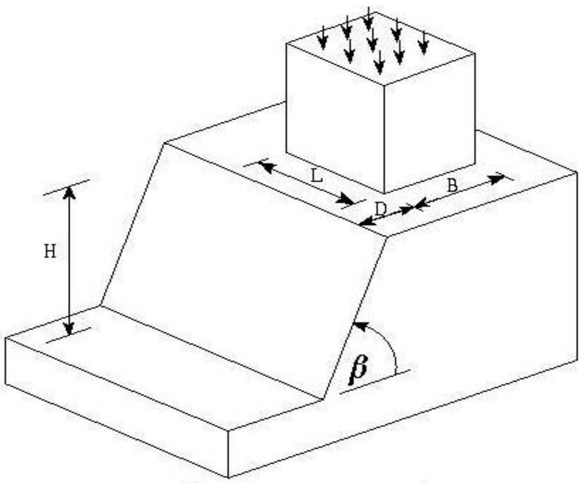

$$\frac{p}{\gamma B} = f\left[\beta, \frac{D}{B}, \frac{H}{B}, \frac{L}{B}, \frac{c}{\gamma B}\right]$$

Figure 1. Statement of the problem.

To simplify the problem, the soil slope is assumed to be undrained following the Tresca yield criterion with a shear strength c_u ($\Phi = 0$). It would be expected that the solution to the ultimate bearing capacity will be dependent on the soil unit weight γ which affects the overall stability of the slope. This is different from the undrained solution of a surface footing resting on level ground in which the ultimate bearing capacity is independent of the soil unit weight. A normalized bearing capacity $p/\gamma B$ is presented throughout the paper and it is a function of *D/B, L/B* and $c_u/\gamma B$ *(SR)*. In all analyses, slope angle β is equal to 90 degree, surcharge loading (q) is equal to zero and *H/B* is equal to five. The use of *H/B* = 5 is appropriate for "above the toe" failure analyses covered in this paper.

The scope of the study to date has seen nine footing lengths investigated. For each of these L/B only purely cohesive soils were investigated and the strength ratio (*SR*) varied from 1 - 30. For each of these cases the location ratio (D/B) was varied from 0 - 5.

3 FLAC MODEL

A typical mesh for the problem using FLAC3D is shown in Figure 2. By making use of symmetry only half of the mesh is required in the analysis. The boundary conditions of model are important because they ensure that the entire soil mass is modeled accurately despite using a finite mesh. The boundary conditions at the left and right side and back and bottom boundaries are modeled as fixed in the *x,y,z* directions respectively. The front face is fixed only in the x direction to facilitate the half model that we will use. To ensure that the boundary conditions have the required effect, the mesh size must be sufficient to fully encapsulate the failure zone.

Note that the foundation is modeled by applying a vertical downwards velocity at the grid points immediately below the foundation. This enables the footing to be modeled as smooth or rough by changing the fixity of the grid points that the velocity is applied to. In this case the footing was modeled as smooth, so the grid points were fixed in the vertical direction thereby allowing horizontal movement of the grid points. FLAC3D was used to solve the resulting problem. During the computation process, the vertical forces at the footing nodes were summed and the averaged footing pressures calculated.

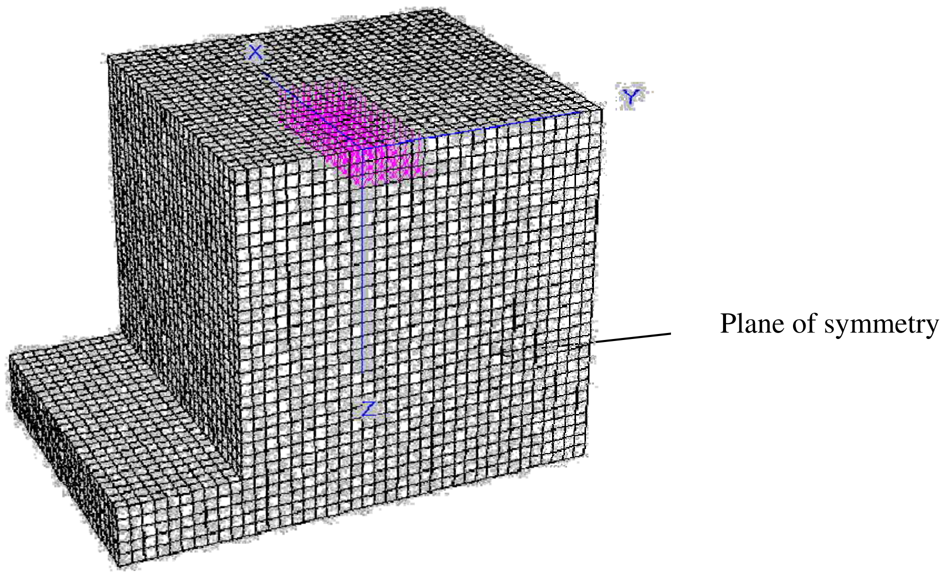

Figure 2. A typical FLAC3D Model for the problem (vertical slope).

4 RESULTS AND DISCUSSIONS

4.1 Effect of D/B

Figure 3 shows the effect of the footing location ratio *D/B* on the normalized bearing capacity p/*γB*. Note that there is an increase in bearing capacity as the footing moves away from the slope. However the rate of increase is dependant upon the footing size (*L/B*) and the strength ratio. For smaller footings (*L/B*=2) there is a significant increase in bearing capacity as the footing is moved away from the slope, resulting in a flat ground failure much sooner than a longer footing (*L/B* > 6). Interestingly, this effect is lessened as the strength ratio decreases (Figure 4). Similarly, as the footing length increases the rate of capacity gain is reduced and hence flat ground failure is reached at a further distance from the slope. Also from Figures 3 and 4 we can see the slight variation in flat ground bearing capacity of the different footing lengths.

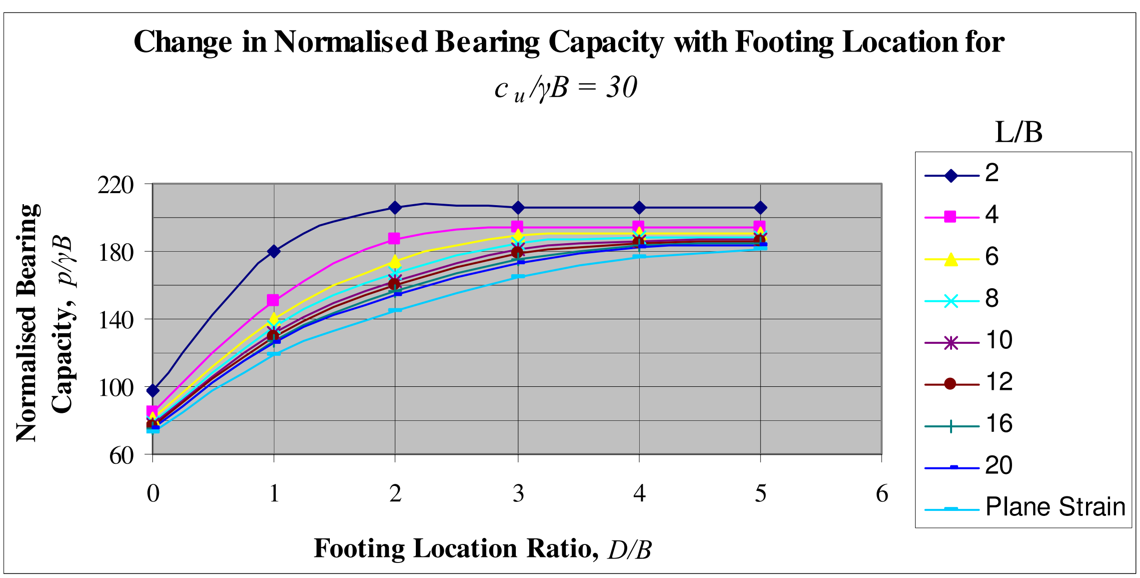

Figure 3. Variation in normalized bearing capacity with footing location for *SR =30.*

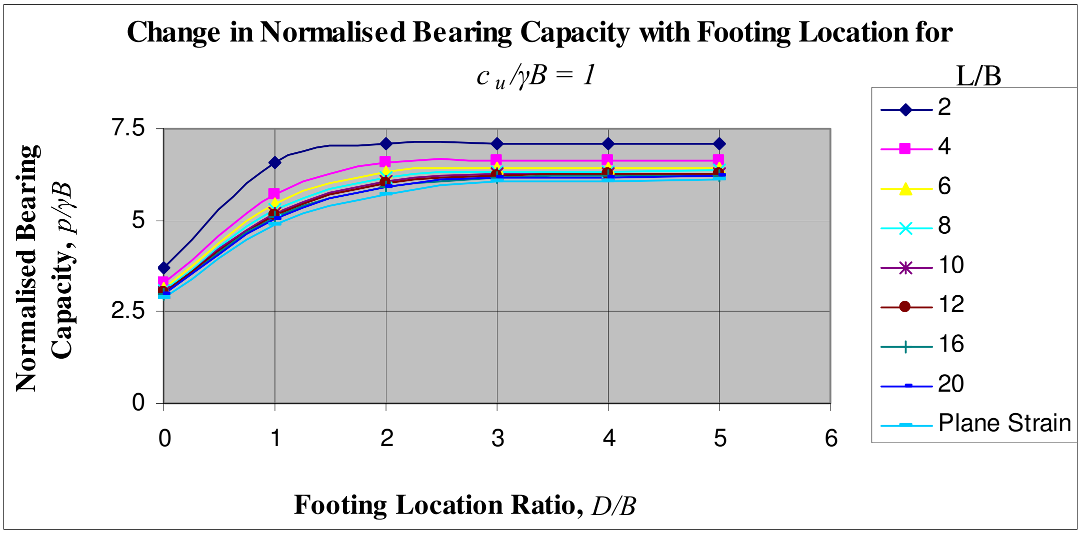

Figure 4. Variation in normalized bearing capacity with footing location for *SR =1*.

Figure 5 shows the velocity contours of four various footing location ratios, *D/B*. Note that the absolute values of these contours are not important for such an idealized material. However these velocity plots show potential failure mechanisms and could be useful for engineers to enhance his or her confidence in design. For the case with *D/B* = 4, a two way failure mechanism is obtained, indicating that the footing capacity is independent of the slope.

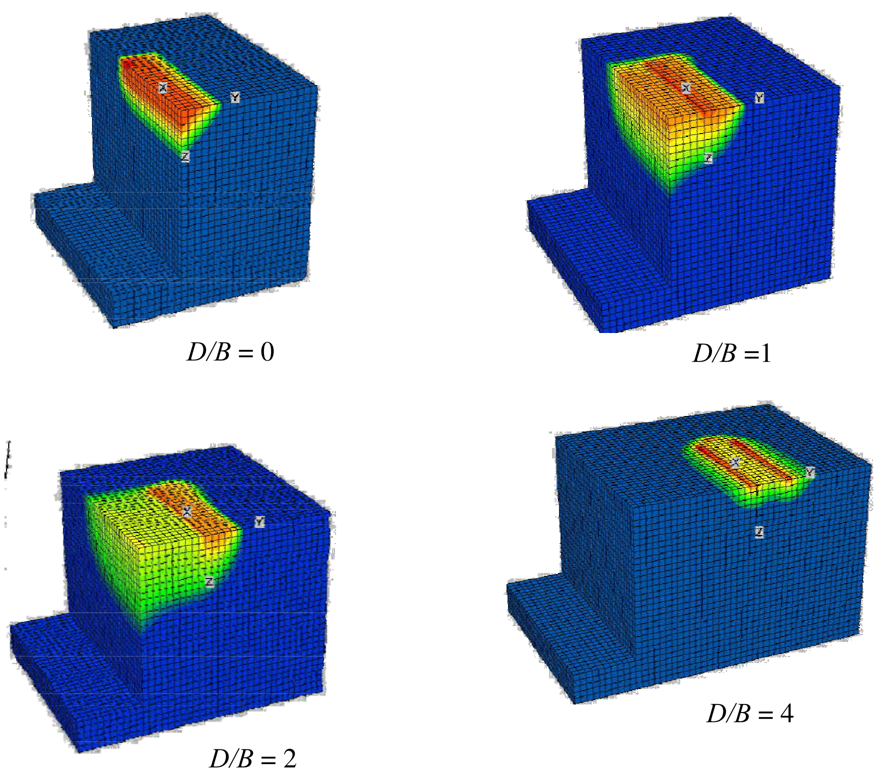

Figure 5. Plot of velocity contours for various D/B (*L/B* = 4 and SR=10)

4.2 Effect of L/B

Figure 6 shows the study of the effects of various footing lengths (*L/B*). Interestingly, we can see that the bearing capacity decreases as the parameter *L/B* increases. It further indicates that the age old use of a plane strain model to determine the bearing capacity of a footing on slope problem provides us with an underestimation of the final bearing capacity of the slope. This means that the plane strain model is conservative. Similar to the study of *D/B*, the effect in bearing capacity reduction is lessened as the strength of the soil mass is decreased, i.e. decreasing *SR*.

Similar conclusions are observed in Figures 7 and 8 where results of *D/B* = 2 and 5 are presented.

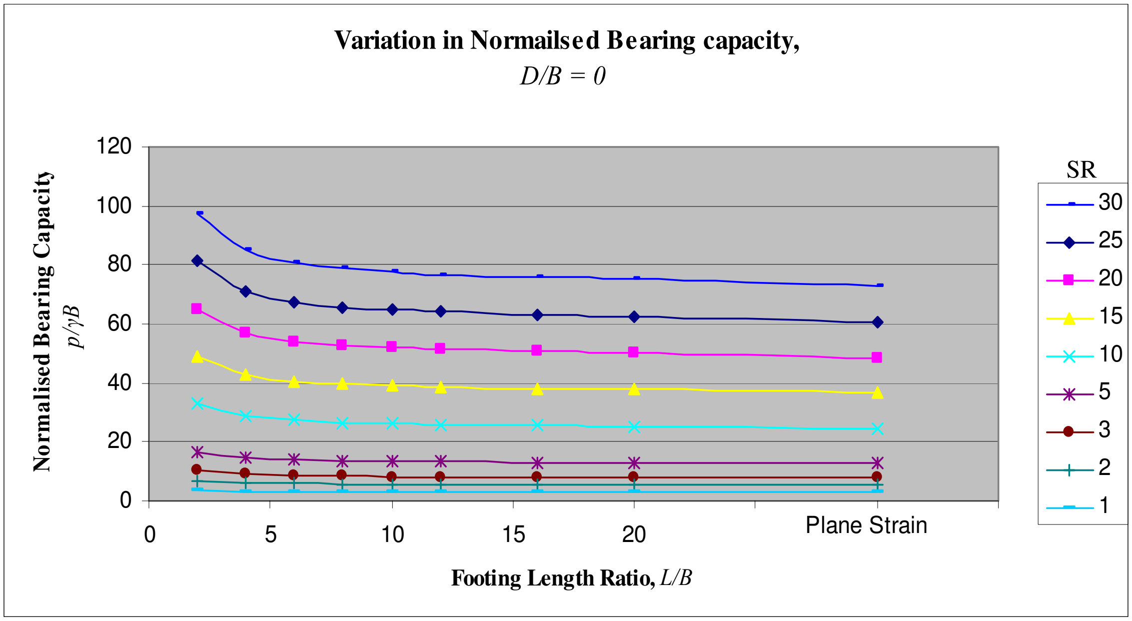

Figure 6. Variation in normalized bearing capacity with footing length for *D/B = 0.*

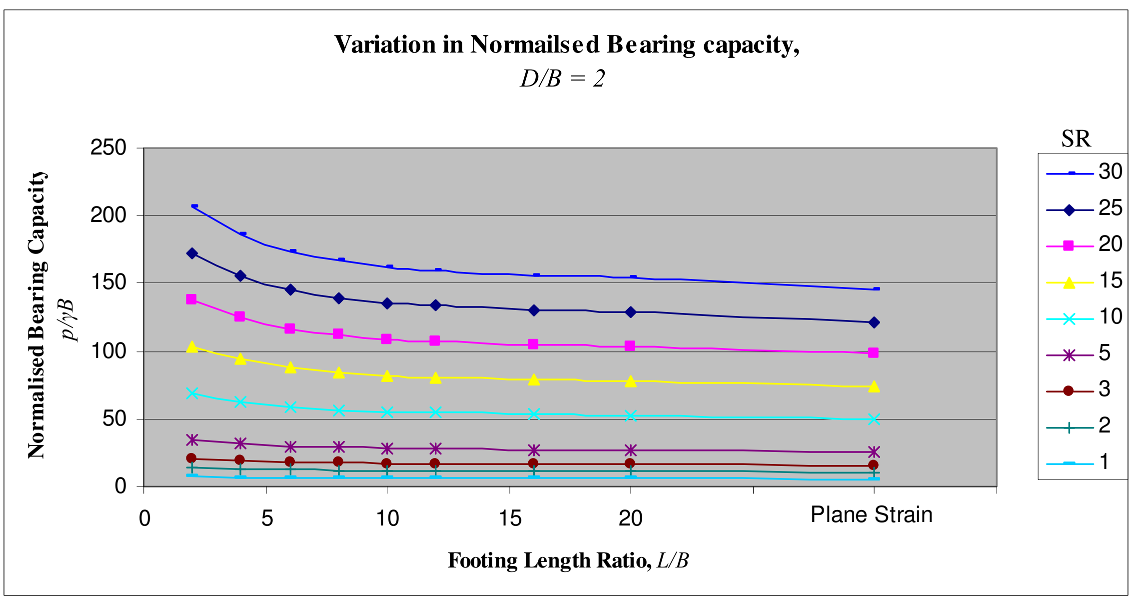

Figure 7. Variation in normalized bearing capacity with footing length for *D/B = 2.*

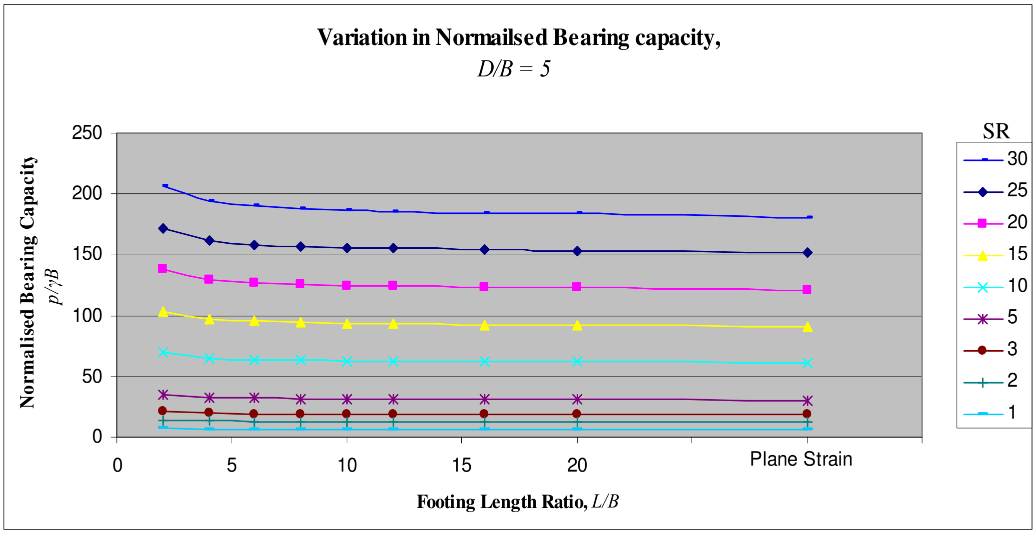

Figure 8. Variation in normalized bearing capacity with footing length for *D/B = 5.*

What this means in terms of practical applications is that the use of a Plane Strain model will give conservative results, the extent of which varies depending on the footing position (*D/B*), the footing length (*L/B*) and the strength of the soil mass (SR).

Figure 9 shows the contour plots of velocity fields for various values of *L/B* (*D/B*=2 and SR=10). Owing to the 3D effects, the blocks slide differently from those in 2D analysis (Shiau et al. 2008). For the small footing (*L/B*=2), a 3D flat ground failure mechanism is obtained. On the other hand, a 3D plane strain model yields a mechanism that is identical to 2D plane strain analysis. For the intermediate cases, the slip planes generated in the x direction (Figure 9) add additional shear strength to the system and thus increases the 3D bearing capacity.

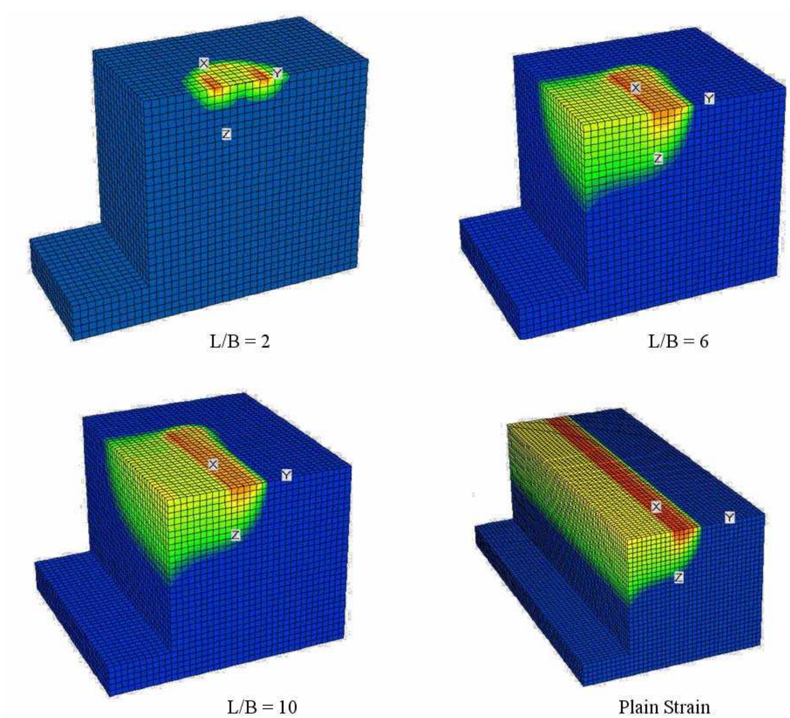

Figure 9. Plot of velocity contours for various L/B (*D/B*=2 and SR=10).

4.3 Effect of Strength Ratio (SR)

The effect of increasing the strength ratio of the footing results in a linear increase in the bearing capacity of the slope. This strength gain is dependent upon the distance away from the slope (*D/B*), as shown Figure 10. There is a clearly defined difference between each of the footing positions. However, as we begin to change the length of the footing by decreasing *L/B* the differentiation between the footing positions becomes less defined. What this means is that a flat ground failure mechanism develops at smaller *D/B* ratios when the length of the footing is decreased. This effect is shown in Figures 9 and 11.

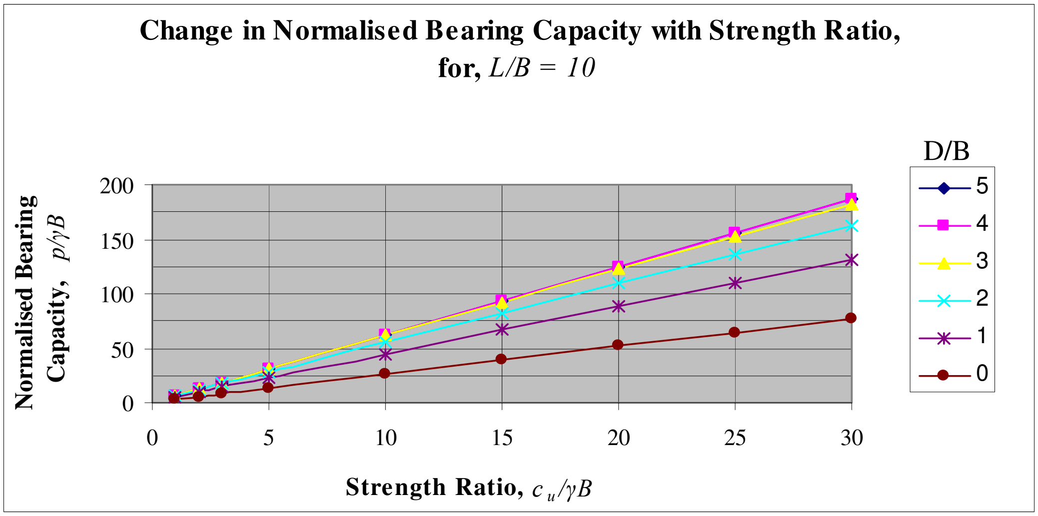

Figure 10. Variation in normalized bearing capacity with strength ratio for *L/B = 10.*

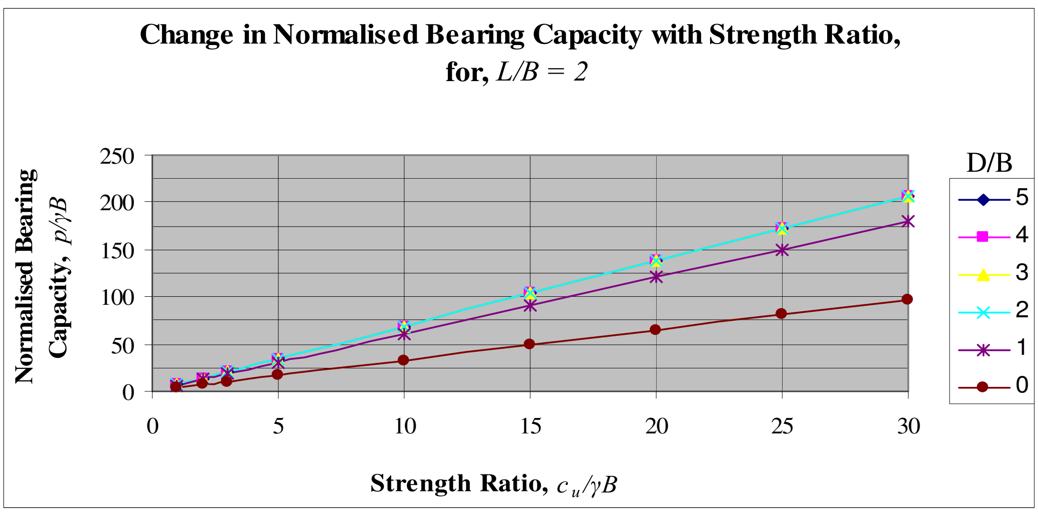

Figure 11. Variation in normalized bearing capacity with strength ratio for *L/B = 2.*

5 CONCLUSIONS

The paper involves the development and verification of numerical models for 3D foundations located near excavation sites. The numerical models created investigated situations of various footing locations. 3D bearing capacity results were compared with those in plane strain 2D analyses. Results were prepared in the form of a dimensionless bearing capacity factor and design charts are presented. The investigation undertaken has shown that FLAC3D is a suitable tool for analyzing these geotechnical stability problems. Future work includes the study of 30 and 60 degree slopes, the effect of slope height (H/B) and the effect of footing roughness.

REFERENCES

de Buhan P. and Garnier D. (1998). "Three dimensional bearing capacity analysis of a foundation near a slope." Soils and Foundations, Vol. 38, No. 3, pp. 153-163.

Kusakabe, O., Kimura T. and Yamaguchi, H. (1981) "Bearing capacity of slopes under strip loads on the top surface." Soils and Foundations, 21(4), 29-40.

Meyerhof, G. G. (1957). "The ultimate bearing capacity of foundations on slopes." Proceedings, 4th International Conference on Soil Mechanics and Foundation Engineering, Vol. 1, 384-386.

Narita, K. and Yamaguchi, H. (1990). "Bearing capacity analysis of foundations on slopes by use of log-spiral sliding surfaces. " Soils and Foundations, 30(3), 144-152.

Shiau, J. S. and Watson, S. F. (2008) "Foundation located near slope ~ A FLAC study." 1st International FLAC/DEM Symposium on Numerical Modeling. Minneapolis. USA.

Shields, D., Chandler N. and Garnier, J. (1990). "Bearing capacity of foundations in slopes" Journal of Geotechnical Engineering, ASCE, 116(3), 528-537.